A Small Interfering CD147-Targeting RNA Inhibited the Proliferation, Invasiveness, and Metastatic Activity of Malignant Melanoma

Xiang Chen,[1] Jing Lin,[1] Takuro Kanekura,[2] Juan Su,[1] Wei Lin,[1] Hongfu Xie,[1] Yixi Wu,[1] Juan Li,[1] Mingliang Chen,[1] and Jing Chang[1]

[1]Department of Dermatology, XiangYa Hospital, Central South University, Changsha, Hunan, China and [2]Department of Dermatology, Field of Sensory Organology, Graduate School of Medical and Dental Sciences, Kagoshima University, Kagoshima, Japan

Abstract

CD147 plays a critical role in the invasive and metastatic activity of malignant melanoma cells by stimulating the surrounding fibroblasts to express matrix metalloproteinases and vascular endothelial growth factor. We developed a system that blocks CD147 in the human malignant melanoma cell line, A375, using RNA interference. By transfecting melanoma cells with the small interfering RNA (siRNA) that targets human CD147, we were able to establish two stable clones in which CD147 expression was significantly down-regulated. This resulted in the decreased proliferation and invasion of A375 cells *in vitro*. CD147 siRNA also down-regulated the expression of vascular endothelial growth factor in these cells and reduced the migration of vascular endothelial cells. The reduction in the CD147 level suppressed the size of s.c. tumors and the microvessel density in an A375 s.c. nude mouse xenograft model. In addition, the *in vivo* metastatic potential of A375 cells transfected with CD147 siRNA was suppressed in a nude mouse model of pulmonary metastasis. (Cancer Res 2006; 66(23): 11323-30)

Introduction

Malignant melanoma, one of the most malignant cutaneous tumors, is characterized by its high potential for invasiveness and metastasis. CD147, a transmembrane glycoprotein of the immunoglobulin superfamily, is expressed in various embryonic and adult tissues (1, 2). The interaction of a molecule identical to CD147, extracellular matrix metalloproteinase inducer (EMMPRIN), with fibroblasts stimulates the expression of matrix metalloproteinases (MMP), and results in the degradation of different components of the extracellular matrix (3, 4). We previously showed that CD147 was highly expressed in malignant melanoma cells, that it interacted with surrounding fibroblasts to stimulate their production of MMP-1, MMP-2, MMP-3, and MT1-MMP, which play an important role in tumor invasiveness and metastasis, and that antibody to CD147 significantly inhibited the production of MMPs by fibroblasts and the invasiveness of melanoma cells (5). Tang et al. (6) reported an EMMPRIN-MMP–vascular endothelial growth factor (VEGF) system in which tumor cell–associated EMMPRIN stimulated tumor angiogenesis by elevating the level of MMPs and VEGF in both tumor and stromal compartments. These findings indicate that CD147 is closely correlated with the progression of malignant melanoma.

RNA interference (RNAi) is a process of sequence-specific posttranscriptional gene silencing initiated by double-stranded RNA (dsRNA) homologous with the target gene. Previous studies elucidated the molecular mechanisms underlying RNAi. dsRNA introduced into cells is processed by Dicer, a cellular RNA polymerase III (RNase III) that cleaves to generate duplexes of 21 to 23 nucleotides with two base-3′ overhangs (small interfering RNA, siRNA), and can extend up to several hundred nucleotides. Thus, RNAi mediates sequence-specific mRNA degradation and exerts an interfering effect (7, 8). RNAi, a conserved process operative in insects, nematodes, plants, and mammalian cells, represents an evolutionary technology that has been adopted in functional genomic analyses, cellular signaling pathway studies, and the development of highly specific gene-silencing therapies to treat tumors and virus infections (8–10). siRNA expression mediated by a vector system named pSUPER enables efficient and specific down-regulation of gene expression in mammalian cells and the maintenance of stable loss-of-function phenotypes of the target gene (11).

We used RNAi technology to knock down the expression of CD147 in A375 melanoma cells in our effort to explore the role and mechanisms of CD147 in the progression of malignant melanoma. We examined the phenotypic changes resulting from the reduction in CD147 expression, including the mRNA and protein levels of CD147 and VEGF, and the proliferative, invasive, angiogenic, and metastatic potential of transfected A375 cells both *in vitro* and *in vivo*. We also studied its effect on the activity of vascular endothelial cells.

Materials and Methods

Cell culture. The human malignant melanoma cell line, A375, was kindly provided by the Shanghai Institute for Biological Sciences of China. Endothelial cells derived from human umbilical vein (ECV-304) were provided by Central South University of China. We prepared normal human fibroblasts (NHFB) from the dermis of a healthy subject. All cells were cultured in DMEM supplemented with 10% FCS, 10^5 units/L penicillin G, and 100 mg/L streptomycin at 37°C in a humidified atmosphere containing 5% CO_2. All human materials were obtained from donors who provided prior informed consent for the use of their materials in this study.

Construction of short hairpin RNA targeting CD147. Based on the CD147 cDNA sequence in GenBank, we used BLAST to design a pair of 64-nucleotide oligos containing endonuclease restriction sites at both ends. Synthesis was at Shanghai Pharmnet Biotechnologies (Shanghai, China). The sequences used were: sequence 1-1, 5′-GATCCCCGTCGTCAGAACACATCAACTTCAAGAGAGTTGATGTGTTCTGACGACTTTTTGGAAA-3′; sequence 1-2, 5′-AGCTTTTCCAAAAAGTCGTCAGAACACATCAACTCTCTTGAAGTTGATGTGTTCTGACGACGGG-3′; sequence 2-1, 5′-GATCCCCTGACAAAGGCAAGAACGTCTTCAAGAGAGACGTTCTTGCCTTTGTCATTTTTGGAAA-3′; sequence 2-2, 5′-AGCTTTTCCAAAAATGACAAAGGCAAGAACGTCTCTCTTGAAGACGTTCTTGCCTTTGTCAGGG-3′.

Note: X. Chen and J. Lin contributed equally to this work.
Requests for reprints: Xiang Chen, Department of Dermatology, XiangYa Hospital, Central South University, XiangYa Road, Changsha, Hunan 410008, China. Phone: 86-731-432-7128; Fax: 86-731-432-8478; E-mail: chenxck@yahoo.com.

doi:10.1158/0008-5472.CAN-06-1536

Oligos were annealed and ligated with linearized pSUPER using T4DNA ligase. The recombinant plasmids were named pSUPER/CD147 siRNA; they were sequenced and identified by PCR and restriction endonuclease digestion.

Transfection of siRNA. A375 cells were seeded (2×10^5 cells/well) in six-well plates. After 24 hours of incubation, they reached 90% to 95% confluence and were transfected with recombinant plasmid pSUPER/CD147 short hairpin RNA (shRNA) or empty vector in serum-free medium using LipofectAMINE 2000 (Invitrogen, Carlsbad, CA). Each plasmid and empty vector (8 μg) and 10 μL of LipofectAMINE 2000 were diluted in serum-free medium (250 μL), left at room temperature for 5 minutes, mixed immediately, and incubated for 20 minutes at room temperature. The mixture was then added to washed A375 cells, and after 5 hours of incubation, the medium was replaced with full medium. Selection with 0.5 μg/mL of puromycin (Sigma-Aldrich Corp., St. Louis, MO) in full medium was started 48 hours after transfection, the medium was replaced 24 hours later, and then every second day. After selection for ~7 to 10 days, the cells were maintained with 0.25 μg/mL of puromycin. Single puromycin-resistant colonies were then isolated and cultured in 24-well plates for subsequent study. A375 cells transfected with empty vector, vector containing sequence 1, and vector containing sequence 2 were designated A375 vector, C1, and C2, respectively.

Semiquantitative reverse transcription-PCR of CD147. Primer pairs designed to amplify CD147 and β-actin were synthesized by Shanghai Pharmnet Biotechnologies. The sequences used were: CD147 primer, sense, 5′-GCAGCGGTTGGAGGTTGT-3′; antisense, 5′-AGCCACGGATGCCCAG-GAAGG-3′; β-actin primer; sense, 5′-GGGCGCCCCAGGCACCA-3′; antisense, 5′-CTCCTTAATGTCACGCACGATTT-3′. Total cellular RNA was extracted using TRIzol reagent (Invitrogen) and reverse-transcribed with a reverse transcription kit (Invitrogen). We used 2 μL of each reaction for PCR in 1 μL of sense and antisense primers, and 1 μL of β-actin primer, 2.5 μL of $MgCl_2$ (25 mmol/L), 1 μL of deoxynucleotide triphosphates, 2.5 μL of 10× PCR buffer, 5 units of Taq DNA polymerase, and 14 μL of double-distilled water in a 25 μL reaction volume. The cycling variables were: one 4-minute cycle at 94°C, 36 cycles at 94°C for 50 seconds, 59°C for 1 minute, 72°C for 50 seconds; final extension was at 72°C for 10 minutes. PCR products (1 μL) were electrophoresed on 1.5% agarose gels and the gray scale ratio of CD147/β-actin was calculated. The clone with the highest inhibition of CD147 expression was selected for further studies.

Western blotting of CD147. Confluent 150 cm^2 flasks of tumor cells were washed thrice with ice-cold PBS, then lysed in buffer [50 mmol/L Tris-HCl (pH 8.0), 150 mmol/L NaCl, 100 μg/mL phenylmethan-sulfonylfluoride, and 1% Triton X-100] for 30 minutes on ice. After removal of cell debris by centrifugation (12,000 × *g*, 5 minutes), the concentration of protein in the supernatant was measured by the bicinchoninic acid protein assay reagent (Pierce Chemical, Co., Rockford, IL) according to the manufacturer's suggestions. Equal amounts (50 μg) of proteins were boiled for 10 minutes in sample buffer and were separated by 12% SDS-PAGE and transferred to a nitrocellulose membrane. Nonspecific reactivity was blocked in 5% nonfat dry milk in TBST [10 mmol/L Tris-HCl (pH 7.5), 150 mmol/L NaCl, and 0.05% Tween 20] for 1 hour at room temperature. The membrane was then immunoblotted with mouse anti-CD147 antibody (1:1,000; Changdao Biotech Corp, Shanghai, China) overnight at 4°C followed by reaction with goat anti-mouse antibody linked to horseradish peroxidase (1:10,000; Santa Cruz Biotechnology, Inc., Santa Cruz, CA). Reactive protein was detected by SuperSignal West Femto trial kit (Pierce Biotechnology, Inc., Rockford, IL) according to the manufacturer's instructions. Each sample was also probed with an anti–glyceraldehyde-3-phosphate dehydrogenase antibody (Sigma-Aldrich Corp.) as a loading control.

Proliferation assays. Tumor cells (2×10^3/200 μL) were plated in 96-well microplates. After 24, 48, and 72 hours of culture, 20 μL of 3-(4,5-dimethylthiazol-2-yl)-2,5-diphenyltetrazolium bromide (MTT) solution (5 mg/mL in PBS) were added, the cells were incubated at 37°C for 4 hours, the supernatant was removed, and 150 μL of DMSO was added to each well. The dark-blue crystals of MTT-formazan were dissolved by shaking the plates at room temperature for 10 minutes and absorbance was then measured on a Bio-Rad Microplate Reader (Bio-Rad, Hercules, CA) using a test wavelength of 490 nm and a reference wavelength of 630 nm. Each experiment was done in triplicate.

Invasion assays. The invasiveness of melanoma cells was assayed using modified transwell Boyden chambers. Polycarbonate filter (pore size, 8 μm) separating the upper and lower compartments was coated with 50 μg of reconstituted basement membrane (Matrigel, Peking University Health Science Center, China). Serum-free DMEM containing 1.0×10^5 cells in 100 μL was introduced into the upper compartment; the lower compartment contained 2×10^5 NHFBs in 100 μL of serum-free DMEM. After 48 hours of incubation at 37°C, cells that had penetrated the Matrigel were quantified by colorimetric MTT assay. Cells on the upper surface of the filter that had not invaded through the Matrigel were removed completely with cotton swabs. Cells that had invaded remained on the filter and 25 μL of MTT solution (5 mg/mL in PBS) were added to each well. After 4 hours incubation at 37°C, the cells on the filter formed dark-blue crystals of MTT-formazan. The filter was then moved to another well containing 150 μL of DMSO to dissolve the formazan crystals. After 15 minutes, the solution containing dissolved formazan was poured into a 96-well microplate and absorbance was measured on a Bio-Rad Microplate Reader using a test wavelength of 490 nm and a reference wavelength of 630 nm. Cells on the polycarbonate filter were fixed with formaldehyde and stained with H&E.

Semiquantitative reverse transcription-PCR of VEGF. Primer pairs designed to amplify VEGF and β-actin were synthesized at Shanghai Pharmnet Biotechnologies. The sequences used were: VEGF primer, sense, 5′-AACCAGCAGAAAGAGGAAAGAGG-3′; antisense, 5′-CCAAAAGCAGGT-CACTCACTTTG-3′; β-actin primer, sense, 5′-GGGCGCCCCAGGCACCA-3′; antisense, 5′-CTCCTTAATGTCACGCACGATTT-3′. Total cellular RNA was extracted with TRIzol reagent (Invitrogen), and reverse-transcribed with a reverse transcription kit (Invitrogen). Extracted RNA (2 μL) was subjected to PCR using 1 μL of sense and antisense primers, 1 μL of β-actin primers, 2.5 μL of $MgCl_2$ (25 mmol/L), 1 μL of deoxynucleotide triphosphates, 2.5 μL of 10× PCR buffer, 5 units of Taq DNA polymerase, and 14 μL of double-distilled water in a 25 μL reaction volume. The cycling variables were: one 4-minute cycle at 94°C, 36 cycles at 94°C for 50 seconds, 55°C for 1 minute, 72°C for 50 seconds; final extension was at 72°C for 10 minutes. PCR products (1 μL) were electrophoresed on 1.5% agarose gels and the gray scale ratio of VEGF/β-actin was calculated.

ELISA assays. NHFBs (2×10^5) and melanoma cells (1×10^5) were plated in six-well plates for culture alone or coculture in complete DMEM. After 24 hours, the culture medium was replaced with fresh serum-free DMEM and the cells were cultured for an additional 48 hours. The culture medium was then replaced with 1 mL of fresh serum-free DMEM. Conditioned medium was collected 3 days later and the concentration of secreted VEGF proteins was determined using an ELISA kit (Jingmei Biotech, Shenzhen, China). Triplicates of each sample were analyzed on a Bio-Rad Microplate Reader.

Endothelial cell migration assays. Endothelial cell migration was evaluated using the QCM-collagen I quantitative cell migration assay kit (Chemicon, Temecula, CA). ECV-304 cells (10^5 in 300 μL serum-free medium) were added to the upper compartment. Serum-free media containing tumor cells as chemoattractants were plated in the bottom compartment. After 6 hours at 37°C, cells that remained in the top compartment were removed with cotton swabs and the filters were stained for 30 minutes with 300 to 500 μL of cell-staining solution (1% crystal violet in acetic acid). The staining solution was eluted for 5 to 10 minutes with 300 μL elution buffer and the number of migrated cells was determined on a Bio-Rad Microplate Reader based on the absorbance of the eluted staining solution; the test wavelength was 490 nm, the reference wavelength 630 nm.

Animal models. All protocols involving animals were reviewed and approved by the ethical review committee of Central South University of China. We used 4- to 6-week-old male BALB/c nude mice (Shanghai SLAC Laboratory Animal Co. Ltd., Shanghai, China). Tumor cells harvested with trypsin-EDTA, washed with DMEM, and resuspended in serum-free DMEM were s.c. inoculated (5×10^6/0.2 mL) into the right axillary fossa. The size of the transplanted tumors was measured every 5 days and the tumor volume was calculated using the formula $V = 1/2 \times (L \times W^2)$. The mice were sacrificed 35 days postinoculation. To determine the metastatic potential of

the cells, we used i.v. inoculation. Suspended cells (1×10^6/0.2 mL) were injected into the lateral tail vein of 4- to 5-week-old mice and they were sacrificed 42 days after inoculation or when they became moribund. At the time of sacrifice, visible tumors and the lungs were excised for histologic examination. Harvested tissues were fixed in 10% buffered formalin, embedded in paraffin, sectioned at 5 μm, and stained with H&E. A minimum of four sections were examined per tissue using light microscopy.

Immunohistochemistry of CD31 and quantification of microvessel density in transplanted tumors. Formalin-fixed paraffin-embedded blocks from the mouse model were collected in this study. For immunohistochemistry, tissue sections (5 μm) were deparaffinized in xylol and rehydrated in graded alcohol. Endogenous peroxidase activity was blocked with 3% H_2O_2 for 30 minutes at room temperature. Sections were then overlaid with antigen retrieval solution [10 mmol/L EDTA (pH 8.0)] to microwave-induced antigen retrieval for 10 minutes at 95°C. Slides were incubated with anti-CD31 antibody (Beijing Biosynthesis Biotechnology Co. Ltd., Beijing, China) overnight at 4°C. Afterwards, tissue sections were subjected to the catalyzed signal amplification system kit (Santa Cruz Biotechnology) according to the manufacturer's instructions. Next, slides were incubated with AEC substrate. The reaction was stopped with distilled water after 5 minutes. After immunohistochemistry, the sections were examined at low magnification (×100) to identify areas with high vessel density. In these areas, the number of microvessels in five high-power fields (×400) was counted. The mean of five fields was computed for each tumor section, and SDs were computed.

Statistical analysis. Data analysis was done by one-way ANOVA. The criterion for significance was $P < 0.05$.

Results

Identification of recombinant plasmid pSUPER/CD147 siRNA. The results of restriction endonuclease-digestion of recombinant plasmids are shown in Fig. 1*A*. When annealed oligonucleotide dsRNAs were ligated with pSUPER, the *Bgl*II site was destroyed. Therefore, the recombinants that originally had a *Hin*dIII site could be linearized with *Hin*dIII but not *Bgl*II. Because linear plasmids are electrophoresed more slowly than circular plasmids, electrophoresis confirmed successful ligation. *Bgl*II-treated circular plasmids electrophoresed faster than *Hin*dIII-treated linear plasmids (Fig. 1*A*, *lanes 3* and *4*). Similar results were obtained when we used simultaneous *Hin*dIII and *Bgl*II digestion (Fig. 1*A*, *lane 5*). Digestion with *Hin*dIII and *Eco*RI yielded a 296-bp dsRNA that contained the insert (Fig. 1*A*, *lane 6*). PCR assays showed that the fragments were correctly inserted (Fig. 1*B*); the sequence of the inserts was identical to that of the synthesized siRNA oligos (Fig. 1*C*).

Semiquantitative reverse transcription-PCR and Western blotting of CD147. Total RNA and protein of A375, A375 vector, C1, and C2 were extracted. The reverse transcription-PCR products were electrophoresed on 1.5% agarose gels, and cell lysates were analyzed for CD147 protein levels by immunoblot analysis with anti-CD147 antibody. As shown in Fig. 2*A*, the PCR product of CD147 was 692 bp, the signal at 537 bp was β-actin, an internal control. In C1, the CD147 signal was barely discernible. The gray scale ratios of CD147/β-actin are shown in Fig. 2*B*. As CD147 was most profoundly inhibited in the C1 clone, we examined another clone transfected with pSUPER/CD147 siRNA1. These two clones were designated as C1a and C1b, and used in further studies. Although the empty vector exhibited no interference effect ($P > 0.05$), transfection with pSUPER/CD147 siRNA1 and siRNA2 resulted in a significant inhibition of CD147 mRNA in the malignant melanoma cell line, A375, by 83.99% in C1a ($P < 0.001$), 83.61% in C1b ($P < 0.001$), and 9.28% in C2 ($P < 0.05$),

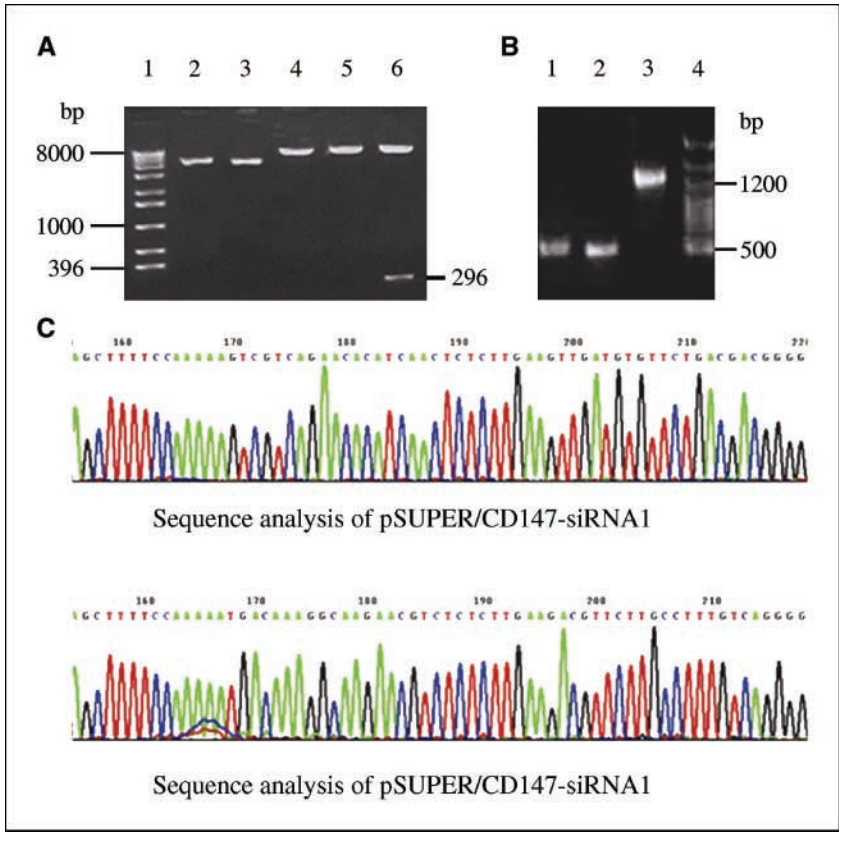

Figure 1. Identification of recombinant plasmid pSUPER/CD147 siRNA. *A,* endonuclease digestion identification: *lane 1,* marker; *lane 2,* recombinant plasmid pSUPER/CD147 siRNA; *lane 3, Bgl*II; *lane 4, Hin*dIII; *lane 5, Hin*dIII and *Bgl*II; *lane 6, Hin*dIII and *Eco*RI. *B,* PCR identification: *lane 1,* sequence 1; *lane 2,* sequence 2; *lane 3,* pSUPER; *lane 4,* marker. *C,* sequence analysis of recombinant plasmids and of the synthesized siRNA oligonucleotides we designed.

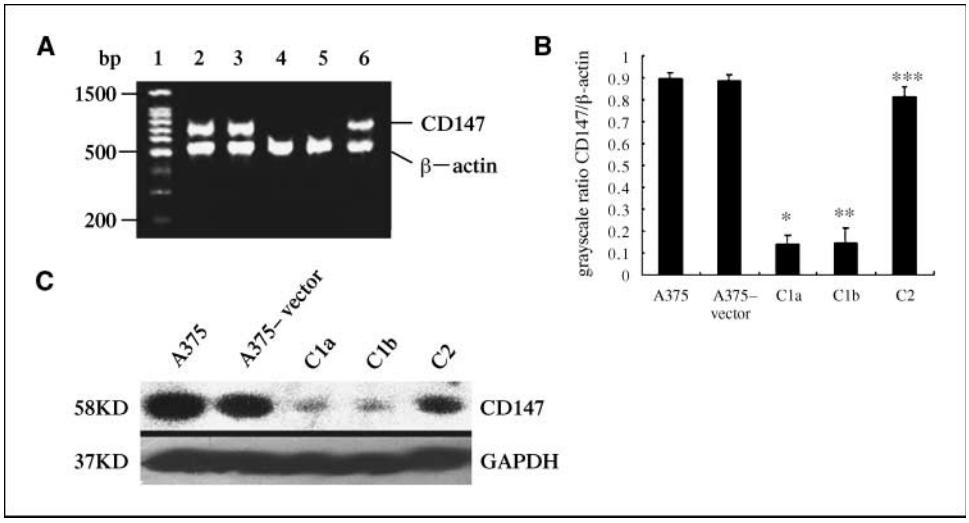

Figure 2. Semiquantitative reverse transcription-PCR and Western blotting of CD147. *A,* reverse transcription-PCR products of total RNA in melanoma cells were electrophoresed on 1.5% agarose gels as described in Materials and Methods. *Lane 1,* marker; *lane 2,* A375; *lane 3,* A375 vector; *lane 4,* C1a; *lane 5,* C1b; *lane 6,* C2. *B,* comparison of gray scale ratio of CD147/β-actin in wild-type melanoma cells (*A375*) and cells transfected with pSUPER (*A375 vector*) or pSUPER/CD147 siRNA (*C1a, C1b,* and *C2*). *, $P < 0.001$; **, $P < 0.001$; ***, $P < 0.05$ compared with A375 (ANOVA). *C,* Western blotting analysis of CD147 protein level after the A375 cells were stably transfected with pSUPER (*A375 vector*) or pSUPER/CD147 siRNA. *Lane 1,* A375; *lane 2,* A375 vector; *lane 3,* C1a; *lane 4,* C1b; *lane 5,* C2.

respectively. As shown in Fig. 2*C*, CD147 protein levels were significantly down-regulated after transfection with CD147 siRNA compared with the untransfected or vector-transfected cells. However, CD147 protein levels in the C1-transfected cells were reduced more strikingly than the C2-transfected cells.

Proliferation assays. Next, we determined the proliferation of A375, A375 vector, C1a, and C1b. As shown in Fig. 3, compared with A375, the proliferation of C1a and C1b was significantly inhibited to 48.54% and 46.60% ($P < 0.05$), 48.29% and 50.24% ($P < 0.01$), and 48.94% and 48.59% ($P < 0.01$) at 24, 48, and 72 hours, respectively. There was no significant difference between A375 vector and A375 ($P > 0.05$).

Invasion assays. To determine the possible role of CD147 siRNA in the invasiveness of melanoma cells we used a transwell invasion assay. A375, A375 vector, C1a, and C1b were placed for 48 hours on Matrigel-coated filters, and then the number of invaded cells was quantified using an MTT assay. CD147 siRNA significantly inhibited the invasiveness of melanoma cells by 50.75% in C1a and by 47.62% in C1b ($P < 0.01$), the empty vector did not ($P > 0.05$; Fig. 4*A*). The filters were stained with H&E and inspected under a microscope. Fewer C1a and C1b than A375 or A375 vector cells exhibited active invasiveness (Fig. 4*B*).

Semiquantitative reverse transcription-PCR of VEGF. The effect of CD147 on VEGF gene expression was analyzed at the mRNA level. Total RNA of A375, A375 vector, C1a, or C1b cells was extracted and the PCR products for VEGF were electrophoresed on 1.5% agarose gels. VEGF and β-actin were detected at 133 and 537 bp, respectively (Fig. 5*A*). The gray scale ratios of VEGF/β-actin of the different cells are calculated (data not shown), and the VEGF mRNA level was reduced by 14.13% in C1a and 15.36% in C1b ($P < 0.05$) compared with A375.

ELISA assays. We previously reported (5) that CD147 expressed on melanoma cells interacted with surrounding fibroblasts to stimulate the production of MMPs. Therefore, we used ELISA to determine whether VEGF production was affected by the coculture of melanoma cells with fibroblasts. We noted a substantial increase in VEGF expression in the coculture medium. The level of soluble VEGF increased by 100.3% ($P < 0.01$) in A375, by 166.6% ($P < 0.01$) in C1a, and by 163.7% ($P < 0.01$) in C1b when these cells were cocultured with NHFB. Compared with A375, the expression of VEGF by C1a and C1b was reduced by 39.3% ($P < 0.01$) and 41.4% ($P < 0.01$), respectively. Compared with A375 cocultured with NHFB, the expression of VEGF by C1a and C1b cocultured with NHFB was reduced by 19.2% ($P < 0.05$) and by 22.8% ($P < 0.05$), respectively (Fig. 5*B*).

Endothelial cell migration assays. The biological activity of VEGF induced by CD147 was determined by the endothelial cell migration assay. Endothelial cell migration in C1a- and C1b-conditioned medium was 55.23% and 58.09% lower compared with A375 medium ($P < 0.01$). A375 vector–conditioned medium manifested no significant inhibitory effect ($P > 0.05$; Fig. 5*C*). Microscopic examination disclosed that fewer endothelial cells migrated in C1a- and C1b-conditioned medium (Fig. 5*D*).

Effects of CD147 knock-down on tumor growth, angiogenesis, and metastasis *in vivo*. We used immunodeficient nude mice to determine the effect of CD147 knock-down on the tumorigenicity, angiogenic potential, and metastatic potential of A375 cells. The transplanted s.c. tumors were excised and their volume was calculated. In mice inoculated with C1a and C1b, the tumor volume

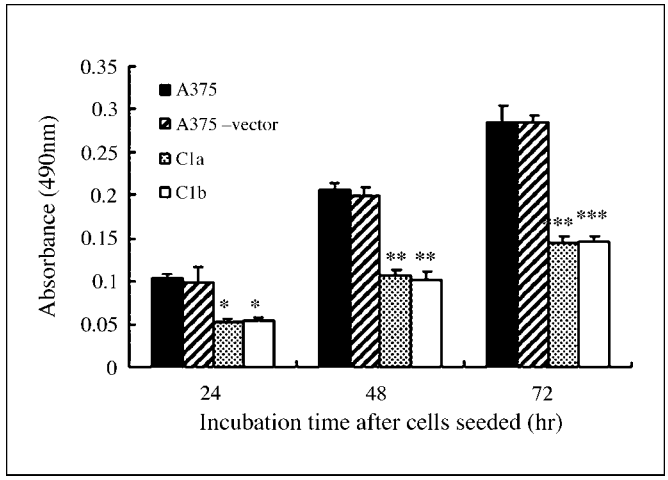

Figure 3. Decrease in the proliferation potential of cells transfected with CD147-targeting siRNA. Melanoma cells (*A375, A375 vector, C1a,* and *C1b*) seeded in 96-well microplates were cultured for 24, 48, and 72 hours and their number was determined by absorbance as described in Materials and Methods. *, $P < 0.05$; **, $P < 0.01$; ***, $P < 0.01$ compared with A375 (ANOVA).

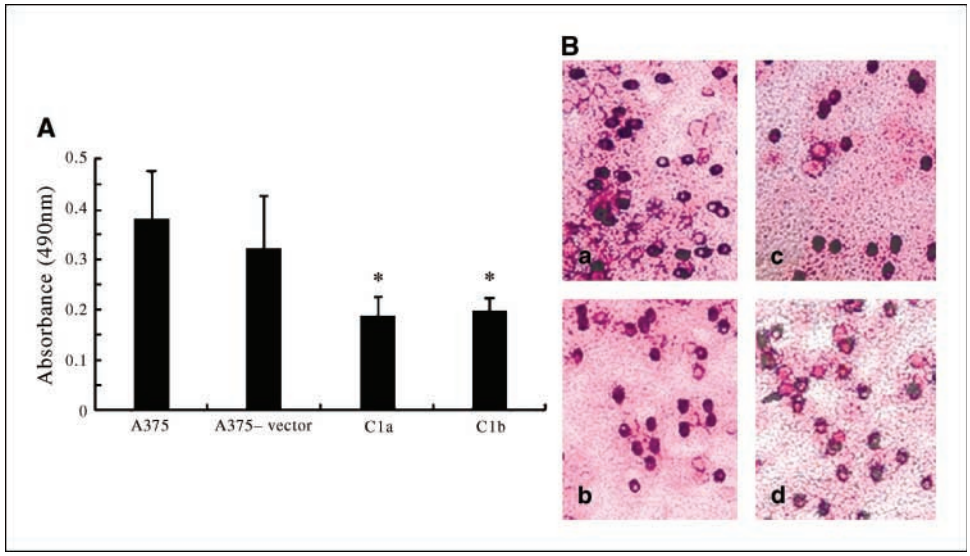

Figure 4. The results of invasion assays. *A,* decrease in the invasiveness of cells transfected with CD147-targeting siRNA. Melanoma cells (*A375, A375 vector, C1a,* and *C1b*) were placed on Matrigel-coated filters in transwell chambers whose lower compartments contained NHFBs. After 48 hours of incubation, invading melanoma cells were identified by absorbance as described in Materials and Methods. *, $P < 0.01$ compared with A375 (ANOVA). *B,* melanoma cells invading a reconstituted basement membrane (Matrigel). The polycarbonate filters were fixed with formaldehyde and stained with H&E: (*a*) A375 (original magnification, ×200); (*b*) A375 vector (original magnification, ×200); (*c*) C1a (original magnification, ×200); (*d*) C1b (original magnification, ×200).

was 46.32% and 50.67% of that recorded for mice transplanted with A375 cells ($P < 0.01$), respectively (Fig. 6*A*). To assess the microvessel density, tumor sections were immunostained with an endothelial cell–specific marker, CD31 (Fig. 6*B*). Quantification of CD31 staining revealed a significantly decreased microvessel density in C1a (6.40 ± 2.30) and C1b (7.03 ± 2.46) tumors compared with A375 (16.37 ± 5.63) or A375 vector (15.83 ± 6.33; $P < 0.01$), respectively. There was larger necrosis in the tumors formed by injecting with C1a and C1b than that of A375 and A375 vector cells (Fig. 6*B*). The incidence of pulmonary tumors reflects the metastatic potential of the injected cells. None of the 12 mice injected with C1a developed lung tumor colonies. On the other hand, 10 of 12 mice treated with A375 and 9 of 12 mice injected with A375 vector manifested lung tumors or became moribund 42 days later (Fig. 6*C*). Histologic study of their lung tissues showed that the pulmonary architecture of mice treated with C1a was normal. However, melanoma cell colonies were present in lung samples from mice injected with A375 (Fig. 6*D*).

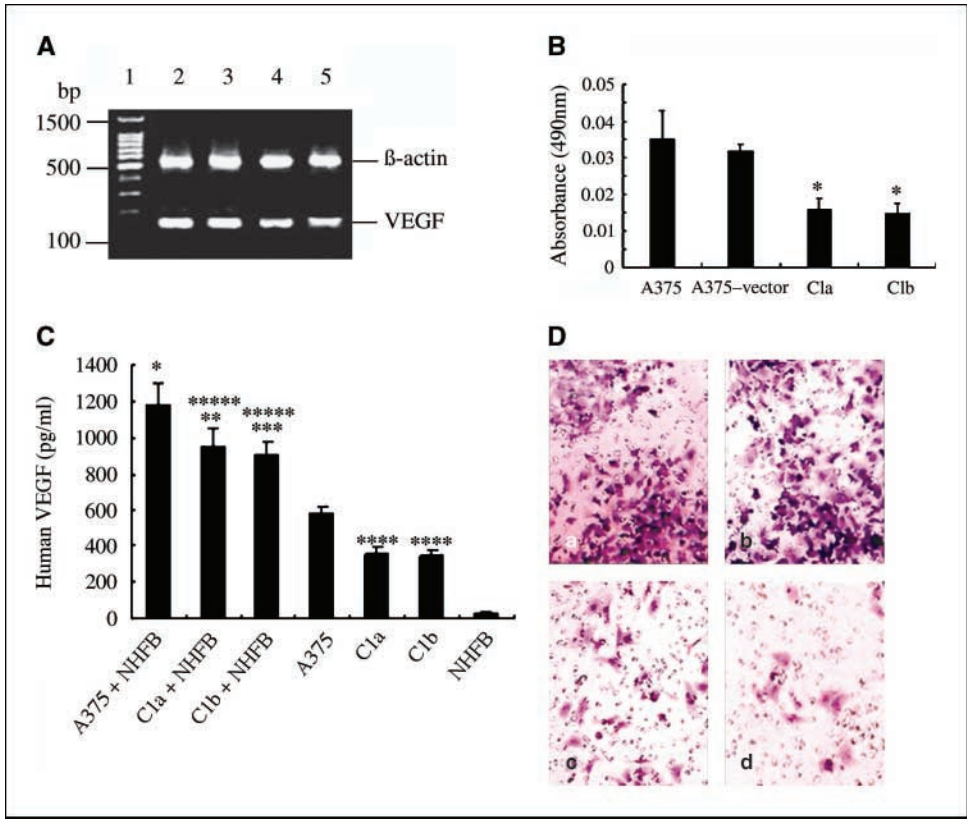

Figure 5. CD147 siRNA can down-regulate the expression of VEGF in A375 cells and those cocultured with fibroblasts and reduce the migration of vascular endothelial cells. *A,* reverse transcription-PCR products of total RNA in melanoma cells were electrophoresed on 1.5% agarose gels as described in Materials and Methods. *Lane 1,* marker; *lane 2,* A375; *lane 3,* A375 vector; *lane 4,* C1a; *lane 5,* C1b. *B,* comparison of VEGF level in A375, C1a, and C1b cells cocultured with or without fibroblasts. *, $P < 0.01$ compared with A375 (ANOVA); **, $P < 0.01$ compared with C1a (ANOVA); ***, $P < 0.01$ compared with C1b (ANOVA); ****, $P < 0.01$ compared with A375 (ANOVA); *****, $P < 0.05$ compared with A375 + NFHB (ANOVA). *C,* decrease in endothelial cell migration induced by CD147-targeting siRNA. Endothelial cells were placed on collagen I-coated filters in transwell chambers whose lower compartments contained melanoma cells (*A375, A375 vector, C1a,* or *C1b*). Their migration was determined by absorbance as described in Materials and Methods. *, $P < 0.01$ compared with A375 (ANOVA). *D,* staining (1% crystal violet in acetic acid) of migrated endothelial cells: (*a*) A375 (original magnification, ×200); (*b*) A375 vector (original magnification, ×200); (*c*) C1a (original magnification, ×200); (*d*) C1b (original magnification, ×200).

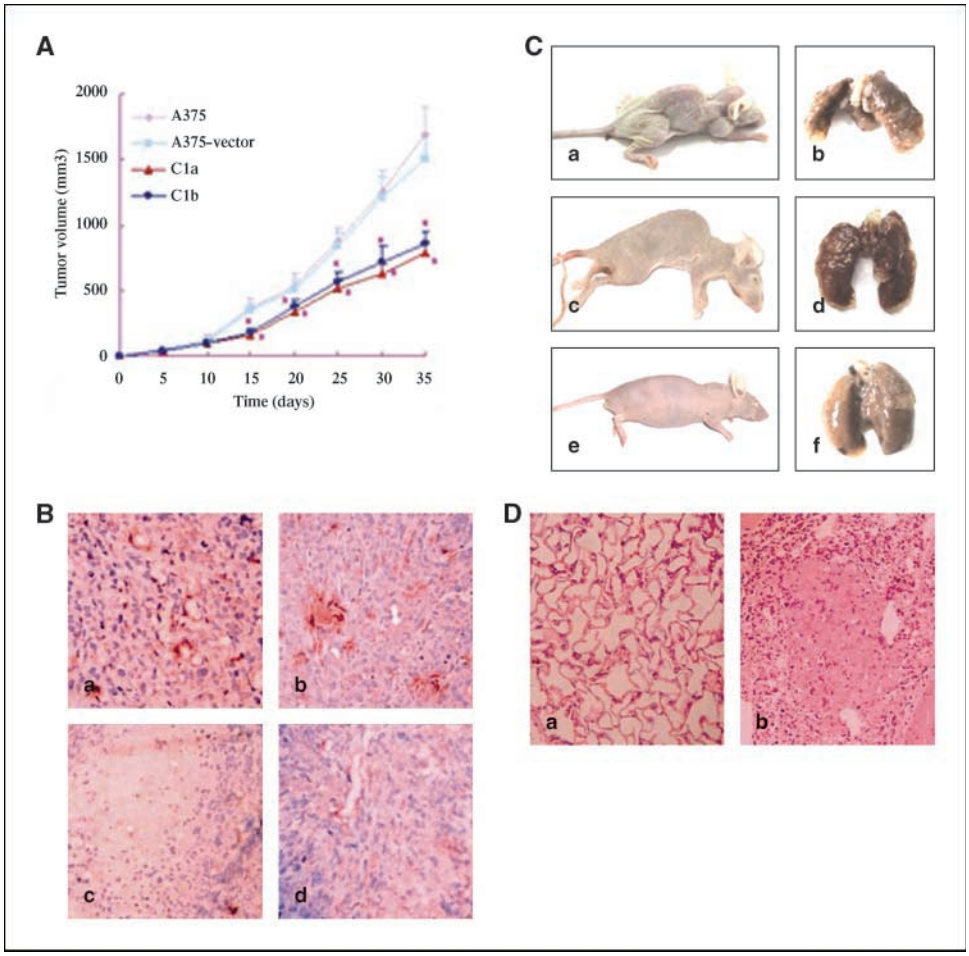

Figure 6. Effects of CD147 knock-down on tumor growth, microvessel density, and metastasis *in vivo*. *A,* the growth curves of transplanted tumors in nude mice. Melanoma cells were injected s.c. into the right axillary fossa and the size and volume of the transplanted tumors were measured in six mice as described in Materials and Methods. *, $P < 0.01$ compared with A375 (ANOVA). *B,* immunohistochemical analysis of CD31-positive microvessels in transplanted tumors: (*a*) A375 (original magnification, ×400); (*b*) A375 vector (original magnification, ×400); (*c*) C1a (original magnification, ×400); (*d*) C1b (original magnification, ×400). *C,* mice were injected i.v. with melanoma cells to determine their metastatic activity. Mice injected with C1a developed no lung tumor colonies. On the other hand, mice injected with A375 or A375 vector developed many lung tumors and were cachectic: (*a* and *b*) A375; (*c* and *d*) A375 vector; (*e* and *f*) C1a. *D,* lung tissue sections of mice inoculated i.v. with melanoma cells. The lung tissue of mice injected with C1a was normal, whereas the lung tissue of mice injected with A375 cells manifested melanoma colonies: (*a*) C1a (original magnification, ×100); (*b*) A375 (original magnification, ×100).

Discussion

MMPs, a family of enzymes that degrade various components of the extracellular matrix, play important roles in tissue remolding, tumor invasion, and metastasis (12–15). The interaction between CD147 and MMPs has been reported (3–5, 16–20). Expression of CD147 was enhanced in a variety of human carcinomas and correlated with tumor progression and invasion by inducing the production of MMPs by stromal cells (3, 4, 16–20). In malignant melanomas, CD147 and MMP-9 were expressed in the invasive radial growth phase (21). Our previous study also showed that the expression of CD147 and MMPs was increased in malignant melanoma cells and that CD147 could increase their invasion potential *in vitro* (5).

VEGF, a homodimeric glycoprotein of the platelet-derived growth factor family, is required for physiologic angiogenesis in embryonic development, female reproductive cycling, and wound healing in adults (22–26). In addition, it plays a pivotal role in tumor angiogenesis and lymphangiogenesis which are crucial for tumor growth, invasion, and metastasis (27). VEGF may contribute to the evasion of the host immune response by inhibiting the function of immunologic cells such as dendritic cells and natural killer cells in tumors (28, 29). In addition, VEGF inhibits apoptosis and provides an autocrine survival signal in tumors (30, 31). Its expression is elevated in many cancers including colorectal, breast, and lung cancers, and in other tumors. Its expression level correlates with microvessel density and metastatic spread in some tumor types as well (32–34). VEGF gene expression is up-regulated by a number of growth factors and by hypoxia and acidosis (27, 35–37).

In gene function studies, the specific knock-down of target genes without affecting other genes is critically important. RNAi mediated by siRNA and shRNA is a specific gene-silencing technology. We used this technology to construct the CD147 siRNA expression vector pSUPER/CD147 siRNA for transfection into the malignant melanoma cell line A375. We established two stable C1a and C1b clones that effectively and stably inhibited CD147 mRNA expression. pSUPER/CD147 siRNA1 significantly reduced CD147 mRNA expression, whereas pSUPER/CD147 siRNA2 had little inhibitory effect. We postulate that positional effects (11, 38) and a variance in the secondary structure of the nucleotide sequence at different sites (8, 39) played a role in the different inhibitory effects of the siRNA targeting the same gene.

CD147 plays an important role in growth, development, cell differentiation, and tumor progression. We previously showed (40) that CD147 may be a molecular marker of keratinocyte proliferation and differentiation, and that it is primarily expressed on the adnexal stem cells and hair germ cells of 20-week-old fetal skin, and the basal cells and anagen hair follicular cells of adult skin. We also showed that the expression level of CD147 on melanoma cells correlated with the degree of malignancy of the tumor. CD147 expression was significantly up-regulated in melanoma with metastasis (5). Stonehouse et al. (41) indicated that

CD147-mediated T cell proliferation is associated with other molecules. Thus, CD147 may be a novel molecular marker for low differentiation and high proliferation.

As shown in the present study, interference with CD147 expression suppressed the proliferative potential of melanoma cells. Cyclophilin A was shown to interact with surface signaling receptors to activate ERK1/2 pathways and DNA synthesis, which resulted in mitogenic effects and the repression of apoptosis in various cells including vascular smooth muscle and endothelial cells (42, 43). The expression of CD147 in these cells was significantly increased, suggesting its participation in the process of proliferation as an essential component of the cell surface signaling receptor of cyclophilin A (42, 43). Recently, Li et al. (44) indicated that exogenous cyclophilin A promotes pancreatic cancer cell growth, which may be mediated through the interaction with CD147 and the activation of ERK1/2 and p38 mitogen-activated protein kinases. Xu and Hemler (45) showed a strong association between cell proliferation and the CD147-CD98 cell surface supercomplex which plays a critical role in energy metabolism. Inconsistent with the present results, Zucker et al. showed that transfection of CD147 into breast cancer cells had no effect on cellular proliferation *in vitro* (46). It is possible that inhibition, but not forced expression, of CD147 affects the proliferation of cells that constitutively express CD147.

Tang et al. (6) have shown that in MDA-MB-231 human breast carcinoma cells, CD147 can stimulate VEGF secretion in both tumor and stromal compartments that promote angiogenesis and tumor progression. Here, we showed that VEGF expression was positively correlated with CD147 expression in melanoma cells. CD147 knock down inhibited VEGF expression, resulting in the suppression of tumor progression and microvessel density in transplanted tumors. However, the inhibitory effect of siRNA on VEGF production was limited. In this study, We postulate that tumor angiogenesis is stimulated by elevated levels of tumor cell–derived VEGF as a direct consequence of increased CD147 expression, and is further enhanced by matrix cell–derived VEGF production induced by CD147-mediated tumor-stroma interactions. Several studies on stimulating the production of VEGF through tumor-stroma interactions mediated by CD147 have been carried out. Investigations have shown that tumor cell–derived MMP-2 or MMP-9 could elaborate soluble VEGF from the extracellular matrix (47, 48). Recent findings suggest that MMPs, i.e., membrane type 1 MMP may directly stimulate VEGF expression via the src tyrosine kinase signaling pathway (49). Tang et al. (50) also identified a positive feedback regulatory mechanism of CD147 expression in fibroblast cells and discovered a soluble form of CD147, which suggests a CD147-mediated MMP-dependent signaling events at the tumor and stroma. However, further studies are under way in our laboratories to elucidate the underlying cellular mechanisms.

We documented that CD147 siRNA inhibited the invasiveness of melanoma cells *in vitro* as well as tumor growth, microvessel density, and pulmonary metastasis in nude mice. Our findings show that CD147 is involved in the invasion and metastasis of melanoma cells.

Conclusion. We showed that CD147-targeting siRNA could significantly down-regulate the CD147 mRNA level in melanoma cells and that it inhibited their proliferation, invasiveness, and metastatic activity *in vitro* and *in vivo*. Our findings indicate that highly expressed CD147 on the surface of melanoma cells plays an important role in the invasiveness and metastasis of malignant melanoma. We also showed that the observed CD147-dependent invasion and metastasis might be mediated, at least in part, by MMPs and VEGF whose expression is up-regulated in both melanoma cells and stroma cells. Our findings provide new insights for the development of gene therapy technology to treat patients with malignant melanoma.

Acknowledgments

Received 4/26/2006; revised 8/8/2006; accepted 10/4/2006.

Grant support: National Natural Science Foundation of China 30200248, 30571682 (X. Chen).

The costs of publication of this article were defrayed in part by the payment of page charges. This article must therefore be hereby marked *advertisement* in accordance with 18 U.S.C. Section 1734 solely to indicate this fact.

References

1. Miyauchi T, Kanekura T, Yamaoka A, Ozawa M, Miyazawa S, Muramatsu T. Basigin, a new, broadly distributed member of the immunoglobulin superfamily, has strong homology with both the immunoglobulin V domain and the β-chain of major histocompatibility complex class II antigen. J Biochem (Tokyo) 1990;107:316–23.
2. Kanekura T, Miyauchi T, Tashiro M, Muramatsu T. Basigin, a new member of the immunoglobulin superfamily: genes in different mammalian species, glycosylation changes in the molecule from adult organs and possible variation in the N-terminal sequences. Cell Struct Funct 1991;16:23–30.
3. Biswas C, Zhang Y, DeCastro R, et al. The human tumor cell-derived collagenase stimulatory factor (renamed EMMPRIN) is a member of the immunoglobulin superfamily. Cancer Res 1995;55:434–9.
4. Kataoka H, DeCastro R, Zucker S, Biswas C. Tumor cell-derived collagenase-stimulatory factor increases expression of interstitial collagenase, stromelysin, and 72-kDa gelatinase. Cancer Res 1993;53:3154–8.
5. Kanekura T, Chen X, Kanzaki T. Basigin (CD147) is expressed on melanoma cells and induces tumor cell invasion by stimulating production of matrix metalloproteinases by fibroblasts. Int J Cancer 2002;99:520–8.
6. Tang Y, Nakada MT, Prabakaran K, et al. Extracellular matrix metalloproteinase inducer stimulates tumor angiogenesis by elevating vascular endothelial cell growth factor and matrix metalloproteinases. Cancer Res 2005;65:3193–9.
7. Fire A, Xu S, Montgomery MK, Kostas SA, Driver SE, Mello CC. Potent and specific genetic interference by double-stranded RNA in *Caenorhabditis elegans*. Nature (Lond) 1998;391:806–11.
8. Elbashir SM, Harborth J, Lendeckel W, Yalcin A, Weber K, Tuschi T. Duplexes of 21-nucleotide RNAs mediate RNA interference in cultured mammalian cells. Nature (Lond) 2001;411:494–8.
9. Bass BL. Double-stranded RNA as a template for gene silencing. Cell 2000;101:235–8.
10. Caplen NJ, Parrish S, Imani F, Fire A, Morgan RA. Specific inhibition of gene expression by small double-stranded RNAs in invertebrate and vertebrate system. Proc Natl Acad Sci USA 2001;98:9742–7.
11. Brummelkamp TR, Bernards R, Agami R. A system for stable expression of short interfering RNAs in mammalian cells. Science 2002;296:550–3.
12. Liotta LA, Steeg PS, Stetler Stevenson WG. Cancer metastasis and angiogenesis: an imbalance of positive and negative regulation. Cell 1991;64:327–36.
13. MacDougall JR, Bani MR, Lin Y, Rak J, Kerbel RS. The 92-kDa gelatinase B is expressed by advanced stage melanoma cells: suppression by somatic cell hybridization with early stage melanoma cells. Cancer Res 1995;55:4174–81.
14. Murray GI, Duncan ME, O'Neil P, McKay JA, Melvin WT, Fothergill JE. Matrix metalloproteinase-1 is associated with poor prognosis in oesophageal cancer. J Pathol 1998;185:256–61.
15. Murray GI, Duncan ME, O'Neil P, Melvin WT, Fothergill JE. Matrix metalloproteinase-1 is associated with poor prognosis in colorectal cancer. Nat Med 1996;2:461–2.
16. Bordador LC, Li X, Tool B, et al. Expression of EMMPRIN by oral squamous cell carcinoma. Int J Cancer 2000;85:347–52.
17. Lim M, Martinez T, Jablons D, et al. Tumor-derived EMMPRIN (extracellular matrix metalloproteinase inducer) stimulates collagenase transcription through MAPK p38. FEBS Lett 1998;441:88–92.
18. Muraoka K, Nabeshima K, Murayama T, Biswas C, Koono M. Enhanced expression of a tumor-cell-derived collagenase-stimulatory factor in urothelial carcinoma: Its usefulness as a tumor marker for bladder cancers. Int J Cancer 1993;55:19–26.
19. Polette M, Gilles C, Marchand V, et al. Tumor collagenase stimulatory factor (TCSF) expression and localization in human lung and breast cancers. J Histochem Cytochem 1997;45:703–9.
20. Sameshima T, Nabeshima K, Toole BP, et al. Glioma cell extracellular matrix metalloproteinase inducer

(EMMPRIN) (CD147) stimulates production of membrane-type matrix metalloproteinases and activated gelatinase A in cocultures with brain-derived fibroblasts. Cancer Lett 2000;157:177–84.
21. van den Oord JJ, Paemen L, Opdenakker G, de Wolf-Peeters C. Expression of gelatinase B and the extracellular matrix metalloproteinase inducer EMMPRIN in benign and malignant pigment cell lesions of the skin. Am J Pathol 1997;151:665–70.
22. Carmeliet P, Ferreira V, Breier G, et al. Abnormal blood vessel development and lethality in embryos lacking a single VEGF allele. Nature 1996;380:435–9.
23. Ferrara N, Carver-Moore K, Chen H, et al. Heterozygous embryonic lethality induced by targeted inactivation of theVEGF gene. Nature 1996;380:439–42.
24. Kronenberg HM. Developmental regulation of the growth plate. Nature 2003;423:332–6.
25. Goede V, Schmidt T, Kimmina S, Kozian D, Augustin HG. Analysis of blood vessel maturation processes during cyclic ovarian angiogenesis. Lab Invest 1998;78: 1835–94.
26. Li J, Zhang Y-P, Kirsner RS. Angiogenesis in wound repair. Angiogenic growth factors and the extracellular matrix. Microsc Res Tech 2003;60:107–14.
27. Ferrara N. Vascular endothelial growth factor as a target for anticancer therapy. Oncologist 2004;9:2–10.
28. Gabrilovich D, Ishida T, Oyama T, et al. Vascular endothelial growth factor inhibits the development of dendritic cells and dramatically affects the differentiation of multiple hematopoietic lineages *in vivo*. Blood 1998;92:4150–66.
29. Melder RJ, Koenig GC, Witwer BP, Safabakhsh N, Munn LL, Jain RK. During angiogenesis, vascular endothelial growth factor and basic fibroblast growth factor regulate natural killer cell adhesion to tumor endothelial. Nat Med 1996;2:992–7.
30. Pidgeon GP, Barr MP, Harmey JH, Foley DA, Bouchier-Hayes DJ. Vascular endothelial growth factor (VEGF) upregulates BCL-2 and inhibits apoptosis in human and murine mammary adenocarcinoma cells. Br J Cancer 2001;85:273–8.
31. Bachelder RE, Crago A, Chung J, et al. Vascular endothelial growth factor is an autocrine survival factor for neuropilin-expressing breast carcinoma cells. Cancer Res 2001;61:5736–40.
32. List AF. Vascular endothelial growth factor signaling pathway as an emerging target in hematologic malignancies. Oncologist 2001;6:24–31.
33. Lee JC, Chow NH, Wang ST, Huang SM. Prognostic value of vascular endothelial growth factor expression in colorectal cancer patients. Eur J Cancer 2000;36:748–53.
34. Poon RT-P, Fan S-T, Wong J. Clinical implications of circulating angiogenic factors in cancer patients. J Clin Oncol 2001;19:1207–25.
35. Shweiki D, Itin A, Soffer D, Keshet E. Vascular endothelial growth factor induced by hypoxia may mediate hypoxia-initiated angiogenesis. Nature 1992; 359:843–5.
36. Banai S, Shweiki D, Pinson A, Chandra M, Lazarovici G, Keshet E. Upregulation of vascular endothelial growth factor expression induced by myocardial ischaemia: implications for coronary angiogenesis. Cardiovasc Res 1994;28:1176–9.
37. Fukumura D, Xu L, Chen Y, Gohongi T, Seed B, Jain RK. Hypoxia and acidosis independently up-regulate vascular endothelial growth factor transcription in brain tumors *in vivo*. Cancer Res 2001;61:6020–4.
38. Torgeir H, Mohammed A, Merete TW. Positional effects of short interfering RNAs targeting the human coagulation trigger tissue factor. Nucleic Acids Res 2002; 30:1757–66.
39. Elbashir SM, Lendeckel W, Tuschl T. RNA interference is mediated by 21- and 22-nucleotide RNAs. Genes Dev 2001;15:188–200.
40. Chen X, Kanekura T, Kanzaki T. Expression of Basigin in human fetal, infantile and adult skin and in basal cell carcinoma. J Cutan Pathol 2001;28:184–90.
41. Stonehouse TJ, Woodhead VE, Herridge PS, et al. Molecular characterization of U937-dependent T-cell costimulation. Immunology 1999;96:35–47.
42. Yang H, Li M, Chai H, et al. Effects of cyclophilin A on cell proliferation and gene expressions in human vascular smooth muscle cells and endothelial cells. J Surg Res 2005;123:312–9.
43. Jin ZG, Melaragno MG, Liao DF, et al. Cyclophilin A is a secreted growth factor induced by oxidative stress. Circ Res 2000;87:789–96.
44. Li M, Zhai Q, Bharadwaj U, et al. Cyclophilin A is overexpressed in human pancreatic cancer cells and stimulates cell proliferation through CD147. Cancer 2006;106:2284–94.
45. Xu D, Hemler ME. Metabolic activation-related CD147–98 complex. Mol Cell Proteomics 2005;4:1061–71.
46. Zucker S, Hymowitz M, Rollo EE, et al. Tumorigenic potential of extracellular matrix metalloproteinase inducer. Am J Pathol 2001;158:1921–8.
47. Bergers G, Brekken R, McMahon G, et al. Matrix metalloproteinase-9 triggers the angiogenic switch during carcinogenesis. Nat Cell Biol 2000;2:737–44.
48. Fang J, Shing Y, Wiederschain D, et al. Matrix metalloproteinase-2 is required for the switch to the angiogenic phenotype in a tumor model. Proc Natl Acad Sci U S A 2000;97:3884–9.
49. Sounni NE, Roghi C, Chabottaux V, et al. Upregulation of VEGF-A by active MT1-MMP through activation of Src-tyrosine kinases. J Biol Chem 2004;279:13564–74.
50. Tang Y, Kesavan P, Nakada MT, Yan L. Tumor-stroma interaction: positive feedback regulation of extracellular matrix metalloproteinase inducer (EMMPRIN) expression and matrix metalloproteinase-dependent generation of soluble EMMPRIN. Mol Cancer Res 2004;2:73–80.